Effective interactions between inclusions in complex fluids driven out of equilibrium

Denis Bartolo,[1] Armand Ajdari,[1] and Jean-Baptiste Fournier[1,2]

[1]*Laboratoire de Physico-Chimie Théorique, UMR CNRS 7083, ESPCI, 10 rue Vauquelin, F-75231 Paris Cedex 05, France*
[2]*Fédération de Recherche, FR CNRS 2438 "Matière et Systèmes Complexes," F-75231 Paris Cedex 05, France*

The concept of fluctuation-induced effective interactions is extended to systems driven out of equilibrium. We compute the forces experienced by macroscopic objects immersed in a soft material driven by external shaking sources. We show that, in contrast with equilibrium Casimir forces induced by thermal fluctuations, their sign, range, and amplitude depend on specifics of the shaking and can thus be tuned. We also comment on the dispersion of these shaking-induced forces, and discuss their potential application to phase ordering in soft materials.

I. INTRODUCTION

A prominent issue in soft condensed matter physics is the understanding of the equilibrium phase behavior of mesoscopic particles immersed in complex fluids: colloidal suspensions [1], liquid droplets in liquid crystals [2], inclusions in lipid membranes [3], charged particles in electrolytes [4], ... A standard and fruitful procedure to describe the large scale properties of inclusions in a soft medium consists in integrating out the numerous "solvent" degrees of freedom via ensemble averaging [1,5]. The interaction between the embedded particles is then described by "effective potentials." The latter can modify the genuine interparticles interaction (Coulomb, van der Waals, . . .) or give rise to entirely new effects. For instance, in some (equilibrium) cases, the external objects do not modify the ground state energy of the medium but only alter its thermal-fluctuations spectrum. The resulting entropic effective interaction has consequently an amplitude proportional to the thermal energy $k_{\mathrm{B}}T$ and a range comparable to that of the correlations of the fluctuations of the medium [7,6]. Such fluctuation-induced (i.e., entropic) interactions are commonly referred to as thermal Casimir interactions in analogy with their famous quantum equivalent [8].

More recently, many experimental studies have reported the organization of particles embedded in fluids when the latter are driven out of equilibrium by the application of external fields [9–12]. Extensions of the concepts of "effective potential" and "entropic forces" to out of equilibrium situations have been scarce [12–14]. Indeed effective potentials cannot be simply derived from a free energy in an out-of-equilibrium context, and only the instantaneous force acting on the external objects for a given configuration of the medium can be defined. The effective interactions between the host objects should then strongly depend on the dynamics ruling the temporal evolution of the medium (in contrast to the equilibrium Casimir case).

In this paper, we attempt to extend the paradigm of Casimir effective interactions to objects immersed in soft systems "shaken" by external energy sources that cannot be *a priori* modeled by heat baths. We use a model, detailed in Sec. II, where both the medium and the objects are very simple. (i) The hosting medium is described by a scalar free

field ϕ living in a d-dimensional space ($d=1,2,3$): for instance, ϕ could represent the height profile of a fluid interface ($d=2$) or a contact line ($d=1$) [15], or the angular deviation of the director of a nematic liquid crystal ($d=3$) [16]. (ii) The external objects are two identical rigid parallel plates that enforce a zero field on their surfaces (Dirichlet boundary conditions). Among the numerous possible choices for the shaking sources, we explore three different cases of experimental relevance (cf. Fig. 1): (A) a localized monochromatic shaking, (B) an uniform monochromatic shaking, (C) a spatially uncorrelated colored noise. All these shaking induce effective interactions between the plates, which we characterize in Sec. III by the corresponding average forces, discussing their sign, amplitude and range. We compare these features with those of the usual thermal Casimir effect. The detail of the calculations and a more thorough analysis of the shaking-induced interactions are gathered in Sec. IV. This more technical section also includes some comments on the time dependence and fluctuations of these shaking-
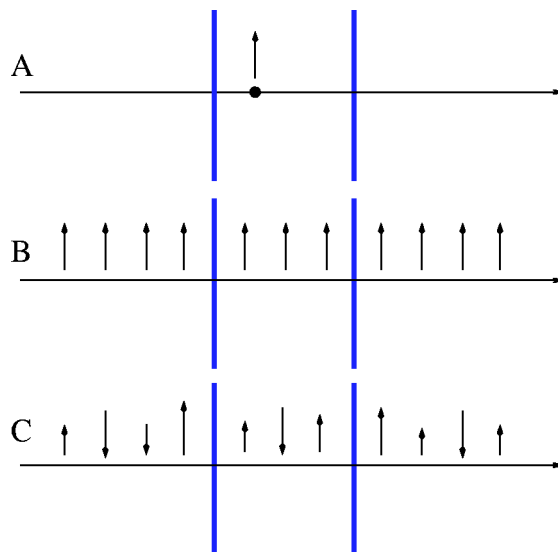

FIG. 1. Sketch of the three shaking processes discussed in the paper: (A) pointlike monochromatic shaking source, (B) uniform monochromatic shaking, and (C) spatially uncorrelated colored noise.
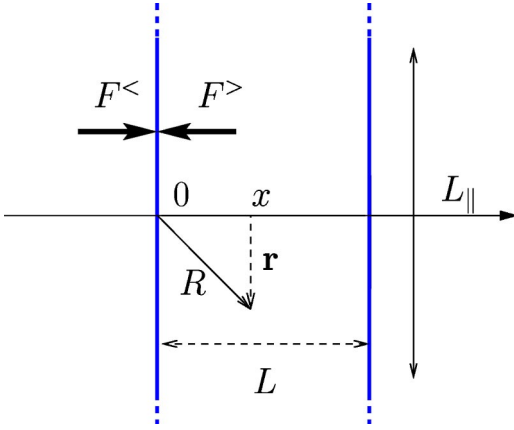
FIG. 2. Two parallel plates, perpendicular to the x axis, separated by a distance L shorter than their lateral extension $L_\parallel$.

induced forces. Section V ends the paper with a synthetic summary of our main results and an outlook on possible applications.

II. MODEL AND NOTATIONS

A. Energetics and force on the plates

We consider two plates in a soft medium separated by a distance L much shorter than their lateral extension $L_\parallel$, as depicted in Fig. 2. Their thickness plays no role in all that follows and will be set to 0. The soft medium is modeled by a scalar field ϕ associated with the elastic Hamiltonian

$$\mathcal{H} = \frac{\kappa}{2} \int d^d \vec{R} [\nabla \phi(\vec{R})]^2, \tag{1}$$

with κ the elastic modulus and $\vec{R} = (x, \mathbf{r})$ where x is the coordinate normal to the plate, see Fig. 2. ϕ is taken dimensionless.

We restrict ourselves to strong plate-field interactions, modeled by Dirichlet boundary conditions (DBC) on the plates: $\phi(x=0, \mathbf{r}) = \phi(x=L, \mathbf{r}) = 0$.

We first focus our attention on the force $F^>$ that the soft medium exerts on the right-hand side of the plate located at $x=0$. For a given configuration of the elastic field, $F^>$ is given by the integral over $\mathbf{r}$ of the stress tensor component $T_{xx}(\mathbf{r})$ [20]. The components T_{ij} of this stress tensor can be obtained by the virtual displacement method taking into account the DBC [6]. In the present geometry, $T_{xx}(\mathbf{r}) = -\frac{1}{2}\kappa[\partial_x \phi(0^+, \mathbf{r})]^2$, so that

$$F^> = -\frac{\kappa}{2} \int d\mathbf{r} [\partial_x \phi(0^+, \mathbf{r})]^2. \tag{2}$$

Note that this force pushes the plate toward the negative x direction whatever the field conformation.

The net force F on the plate is the algebraic sum of the contributions of the two sides: $F \equiv F^> + F^<$. The force $F^<$ is given by a formula similar to Eq. (2), so that

$$F = -\frac{\kappa}{2} \int d\mathbf{r} [\partial_x \phi(0^+, \mathbf{r})]^2 + \frac{\kappa}{2} \int d\mathbf{r} [\partial_x \phi(0^-, \mathbf{r})]^2. \tag{3}$$

B. Dynamics

For the sake of clarity all calculations are performed within the simplest local and strongly dissipative dynamical scheme: the ϕ field evolves under the application of an external "shaking" source η as

$$\gamma \partial_t \phi = -\frac{\delta \mathcal{H}}{\delta \phi} + \eta = \kappa \nabla^2 \phi + \eta, \tag{4}$$

$$\phi(0, \mathbf{r}, t) = \phi(L, \mathbf{r}, t) = 0. \tag{5}$$

Here γ is a generalized friction coefficient.

A description of the dynamics of the plates is beyond the scope of this paper, and we assume that they are fixed. L is thus a constant. After partial Fourier transform with respect to t and $\mathbf{r}$, Eqs. (4) and (5) can be recast into

$$\phi_{\omega,\mathbf{q}}(x) = \int_0^L dx' \mathcal{R}^>_{\omega,\mathbf{q}}(x, x') \eta_{\omega,\mathbf{q}}(x'), \tag{6}$$

where the response function $\mathcal{R}^>$ corresponds to the diffusion kernel in the slab geometry with DBC and with a diffusion constant κ/γ. The Fourier transforms used in this paper are defined by $f_{\mathbf{q}} \equiv \int d\mathbf{r} f(\mathbf{r}) \exp(i\mathbf{q} \cdot \mathbf{r})$ and $g_\omega \equiv \int dt g(t) \exp(i\omega t)$.

A generalization of our results obtained with Eqs. (4) and (5) to other slow dynamics that obey an equation of form (6) with a different kernel will be commented on throughout the text. This generalization is simple provided the dynamic linear response of ϕ relates spatial and temporal scales through an algebraic relation $l_\omega \sim \omega^{-1/z}$, where l_ω is the spatial extension of the elastic distortion resulting from a localized periodic shaking of pulsation ω, and z is the so-called dynamical exponent. The diffusive model described above by Eqs. (4) and (5) indeed fits in this picture with $z=2$ and

$$l_\omega = [(\gamma/\kappa)\omega]^{-1/2}. \tag{7}$$

III. AVERAGE FORCES INDUCED BY THREE KINDS OF SHAKING

To set a reference for further comparison, we first recall the expression of the average thermal force F_{Casimir} on the plate at $x=0$ if the whole medium is thermally excited by a heat bath imposing a temperature T [22]. The simplest derivation consists in computing the total free energy of the system for a given interplate distance L, and taking its derivative with respect to L. An alternative approach is to consider the model Langevin dynamics for the field given by Eqs. (4) and (5), with η a thermal Gaussian white noise of zero mean and of variance $\langle \eta(\vec{R}, t)\eta(\vec{R}', t') \rangle = 2\gamma k_B T \delta(\vec{R} - \vec{R}')\delta(t-t')$. Averaging over realizations of the noise leads to the same universal expression for the net thermal Casimir force [6]

$$F_{\text{Casimir}} = A_d k_B T \frac{L_{\parallel}^{d-1}}{L^d}, \tag{8}$$

with $A_d = (d-1)\Gamma(d/2)\zeta(d)/(4\pi)^{d/2}$. This universal mean force describes a long range attraction that depends on the temperature of the heat bath but not on specific material properties such as κ and γ.

We now calculate the average forces generated by the three nonthermal shaking processes mentioned in the introduction, with a field ϕ that evolves according to Eqs. (4) and (5).

A. Average force induced by a localized monochromatic shaking

We start with the simplest choice for the shaking in Eq. (4), namely, a pointlike monochromatic shaker oscillating at a pulsation ω_s, located at an equal distance $L/2$ from the two plates:

$$\eta(\vec{R},t) = \eta_s a^d \cos(\omega_s t)\delta(x-L/2)\delta(\mathbf{r}), \tag{9}$$

The noise amplitude has been arbitrarily split into the product of a microscopic volume a^d, where the medium is shaken, and a shaking amplitude η_s that has the dimension of an energy density.

Such a process could be, for example, the result of the forcing of a microscopic "active" particle located between the two plates (e.g., a magnetic particle under the influence of an external oscillating magnetic field), in which case a is typically fixed, whereas η_s and ω_s can be externally tuned.

The net force F felt by the plate at $x=0$ reduces to its right hand side contribution $F^>$ since the outer medium remains undistorted [$\phi(x<0)=0$]. Moreover, the geometry is here totally symmetrical so that the force felt by the plate at $x=L$ is $-F$. Denoting $F_A^>$ the time averaged force for this process and anticipating on the detailed discussion of Sec. IV A, we use Eq. (23) to write

$$F_A^> = -\frac{(\eta_s a^d)^2}{\kappa}\frac{1}{L^{d-1}}\Upsilon_A\left(\frac{1}{2},\frac{L}{l_{\omega_s}}\right). \tag{10}$$

Again $l_{\omega_s} = [(\gamma/\kappa)\omega_s]^{-1/2}$ is the dynamical length associated with the shaking pulsation ω_s. The adimensional function $\Upsilon_A(1/2,L/l_{\omega_s})$ is plotted in Fig. 3, and its general expression (including the shaker position dependence) is given below in Eq. (23).

Two different limit regimes can be identified: If $L/l_{\omega_s} \ll 1$, the shaking period is much larger than the relaxation of any interplate field excitation, so that the elastic deformations generated at $x=L/2$ propagate along the x axis up to the plate surfaces. In this quasistatic limit, the time averaged force $F_A^>$ felt by the plate at $x=0$ is comparable to the elastic force on the plates under the application of a constant static "effective" perturbation $1/\sqrt{2}\,\eta_s a^d\delta(x-L/2)\delta(\mathbf{r})$. The latter induces static deformations of lateral extension L on the plate. Thus, $F_A^>$ scales as $\eta_s^2 a^{2d}/(\kappa L^{d-1})$, independent of
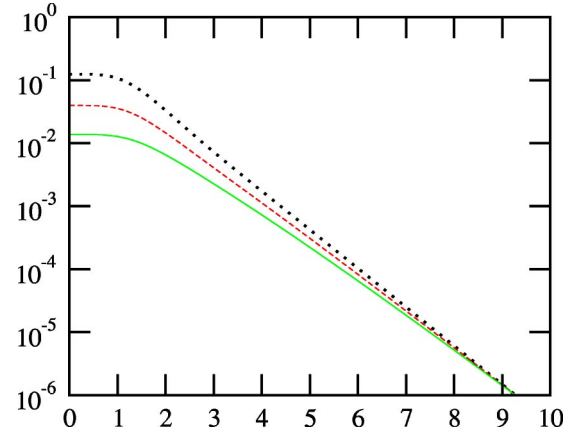

FIG. 3. *Localized monochromatic shaking*. Log-linear plot of the scaling function $\Upsilon_A(1/2,L/l_{\omega_s})$ against $L/l_{\omega_s} = (\gamma/\kappa)^{1/2}\omega_s^{1/2}L$, for various space dimensions: $d=3$ full line, $d=2$ dashed line, and $d=1$ dotted line.

the shaking period. In contrast, the dynamic length is much smaller than the plate-shaker distance if $L/l_{\omega_s} \gg 1$. The elastic deformations are exponentially screened before reaching the plate surfaces. Therefore, the force amplitude decays exponentially, as shown in Fig. 3.

In summary, a localized periodic shaking induces an effective interplate interaction. Although F_{Casimir} is universal and leads to an attraction between the two plates, the interaction obtained here is repulsive and does depend both on the elastic modulus of the surrounding "fluid" and on its dynamics (through l_{ω_s}). Finally, both the range and the amplitude of the present shaking-induced force can be externally tuned by varying the pulsation ω_s and the amplitude η_s of the shaking. The dependence of the force on the shaker position as well as its fluctuations will be discussed in Sec. IV.

B. Average force induced by a uniform monochromatic shaking

We now suppose that the elastic medium is everywhere periodically and homogeneously shaken:

$$\eta(\vec{R},t) = \eta_s\cos(\omega_s t). \tag{11}$$

Possible experimental realizations include the homogeneous and periodic shaking of a metallic elastic line using a magnetic field [17] or the driving of an interface between two dielectric liquids using ac electric fields [18]. One may also use flexoelectric effects in liquid crystal to generate such a shaking process [19]. By symmetry the two plates feel opposite instantaneous forces. The exact expression for the time averaged force F_B on the $x=0$ plate is computed in Sec. IV:

$$F_B = \frac{\eta_s^2 L_{\parallel}^{d-1}}{\kappa}l_{\omega_s}^2\Upsilon_B\left(\frac{L}{l_{\omega_s}}\right). \tag{12}$$

The dimensionless quantity Υ_B, see Eq. (30), is plotted in Fig. 4: it is nonmonotonic and changes sign periodically. Given the plates geometry and the shaking translational in-
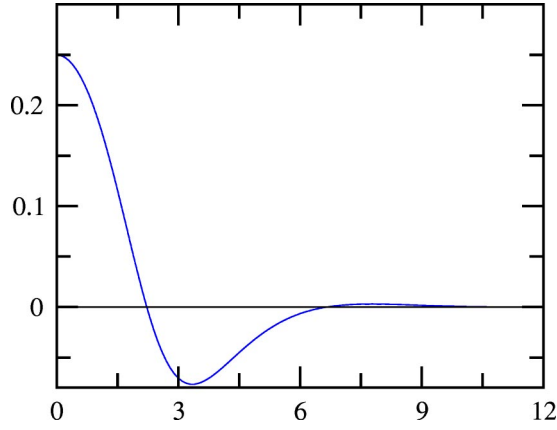
FIG. 4. *Uniform monochromatic shaking*. Linear plot of the scaling function $\Upsilon_B(L/l_{\omega_s})$ as a function of $L/l_{\omega_s} = (\gamma/\kappa)^{1/2}\omega_s^{1/2}L$.

variance, the net normal stress $F_B/L_\parallel^{d-1}$ depends neither on the plates lateral extension $L_\parallel$ nor on the dimension d. The fast and slow shaking asymptotics can thus be qualitatively inferred from dimensional analysis. If the medium is slowly shaken ($L/l_\omega \ll 1$), the net force amplitude diverges as $l_{\omega_s}^2 \sim 1/\omega_s$. First, notice that a constant uniform source η_s between the plates induces an homogenous normal stress on the inner side of the plate ($x=0^+$) that scales necessarily as $F_B^>/L_\parallel^{d-1} \sim \eta_s^2 \kappa^{-1} L^2$. Second, on the left-hand side of the plate ($x<0$), l_{ω_s} is the only length scale available to construct the normal stress $F_B^</L_\parallel^{d-1} \sim \eta_s^2 \kappa^{-1} l_{\omega_s}^2$. In this slow shaking regime this latter contribution dominates, so that Υ_B plateaus to a finite value. Turning now to the $L/l_\omega \gg 1$ limit, if the interplate distance goes to infinity, the two sides of the plate face identical semi-infinite media. Consequently, they are pushed in opposite directions with the same amplitude and thus feel on average no net force. So, in this limit $L/l_\omega \gg 1$ that also corresponds to fast shaking at fixed L, F_B decays to zero, as observed in Fig. 4.

Returning to the most remarkable features, Fig. 4 and Eq. (12) show that the fluctuations of a uniformly shaken medium induce effective interplate forces that strongly differ from F_{Casimir}. They are indeed completely tunable unlike their equilibrium analog. Their sign, amplitude, and range can all be controlled externally by varying the shaking period and amplitude.

C. Average force induced by a stochastic shaking: colored noise

Finally the case of stochastic shaking sources is considered. As mentioned above, if η is the white Langevin noise modeling the coupling to a heat bath, the resulting field fluctuations induce thermal Casimir interactions between the plates. Any other noisy shaking drives the system out of equilibrium. Numerous examples of elastic materials shaken by "active" stochastic processes are provided by biological systems, e.g., active membranes [11], actin-myosin gels [21], etc. Without attempting to describe accurately the specifics of the noise in a given system, we focus here on the simple case of a spatially uncorrelated colored noise of zero mean,
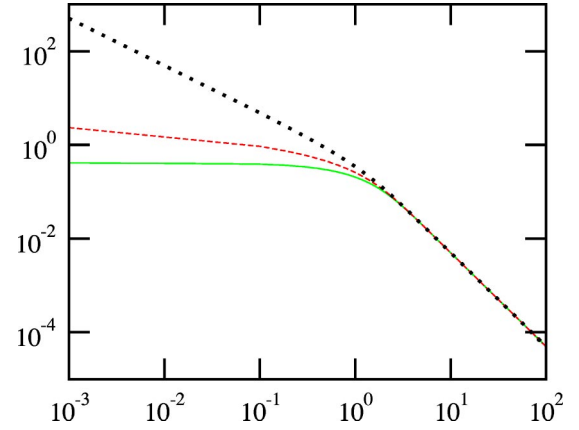

FIG. 5. *Colored noise*. Log-log plot of the ratio $\Upsilon_C(L/l_{\Omega_s})/A_d$ vs $L/l_{\Omega_s} = (\gamma/\kappa)^{1/2}\Omega_s^{1/2}L$. The full line corresponds to $d=3$, the dashed line corresponds to $d=2$, and the dotted line corresponds to $d=1$.

seeking for the influence of its color on the interplate force generated. We describe the fluctuations of this noise by

$$\langle \eta(\vec{R},t)\eta(\vec{R}',t')\rangle = \eta_s^2 a^d S(t-t')\delta(\vec{R}-\vec{R}'), \quad (13)$$

where the correlation $S(t)$ is defined by its Fourier transform S_ω, also referred to as the noise power spectrum:

$$S_\omega = \frac{\Omega_s}{\Omega_s^2 + \omega^2}. \quad (14)$$

In Eq. (13) a is a microscopic distance chosen so that the mean squared noise satisfies $\langle \eta^2(\vec{R},t)\rangle = \eta_s^2$. Again η_s has the dimension of an energy density. The white noise limit corresponds to $\Omega_s \rightarrow \infty$, with $\eta_s^2 a^d \Omega_s^{-1}$ kept constant.

The mean net force F_C on the $x=0$ plate is exactly computed in Sec. IV C:

$$F_C = \frac{\eta_s^2 a^d}{\kappa} \frac{L_\parallel^{d-1}}{L^{d-2}} \Upsilon_C\left(\frac{L}{l_{\Omega_s}}\right). \quad (15)$$

The dimensionless ratio Υ_C/A_d is plotted in Fig. 5, using Eq. (33). We recall that A_d measures the amplitude of the thermal Casimir force $[A_d = (d-1)\Gamma(d/2)\zeta(d)/(4\pi)^{d/2}]$.

Postponing a more involved discussion to the following section, we emphasize here three points. First, the color of the noise has no influence on the sign of the force: the two plates attract each other whatever Ω_s and η_s. Second, Υ_C decreases monotonically with L/l_{Ω_s}, in other words the larger the noise correlation time Ω_s^{-1}, the stronger the force felt by the two plates. Third, Fig. 5 indicates that $\Upsilon_C(u)/A_d$ decays as $1/(2u^2)$ when $u \gg 1$. This implies that the attraction is long ranged and decays only algebraically with the interplate distance. A connection with the Casimir result appears in this regime: if one sets $\eta_s^2 a^d \Omega_s^{-1} = 2\gamma k_B T$, then in the white noise limit $\Omega_s \rightarrow \infty$, F_C converges as expected to $F_{\text{Casimir}} = A_d k_B T L_\parallel^{d-1}/L^d$.
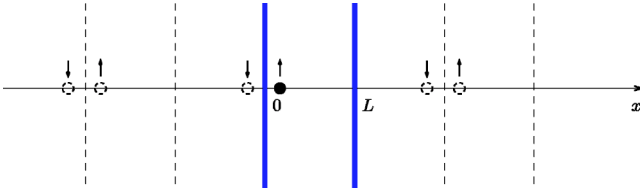
FIG. 6. Distribution of the image sources for the two plates geometry and Dirichlet boundary conditions. The filled circle is the original source and the dashed circles are its mirror images.

To conclude, we have shown that Casimir-like attractions can be induced by colored noisy shaking. These attractions decay algebraically at long distance as in the thermal case and contrary to the two former monochromatic cases. Their amplitudes depend explicitly on the material properties and their scaling on the noise color.

IV. SHAKING-INDUCED FORCES: DETAILED ANALYSIS

In this section we provide a more detailed analysis of the interactions induced by the three kinds of shakings: in addition to the explicit derivation of the average of the corresponding forces, we also comment on their temporal fluctuations.

We start with the derivation of the tool that will allow us to compute the forces on the $x=0$ plate in all situations, namely, the linear response function $\partial_x \mathcal{R}$ of the field's gradient at the surface of the plate to a pointlike shaker in the medium [by definition, the kernel $\mathcal{R}$ is the solution of the dynamic Eqs. (4) and (5), with $\eta(\vec{R},t)=\delta(\vec{R}-\vec{R}')\delta(t-t')$]. We compute this quantity using an image method, which conveys an intuitive picture [23]: as in electrostatics, these equations can be solved replacing the constraint at boundaries (5) by the addition of an *ad hoc* distribution of image sources outside the integration domain.

We consider first a shaking source located in the interplate region $0<x'<L$ and compute the response $\partial_x \mathcal{R}^>$ on the $x=0^+$ side of the plate. In the present slab geometry, the images are the mirror images of the original source through virtual reflecting planes located at $x=nL$, as depicted in Fig. 6. Consequently, the response $\mathcal{R}^>_{\omega,\mathbf{q}}(x,x')$ can be expressed as an infinite sum over all the image contributions:

$$\mathcal{R}^>_{\omega,\mathbf{q}}(x,x')=\sum_{n\in\mathbf{Z}}\mathcal{R}_{\omega,\mathbf{q}}(2nL+x'-x)$$

$$-\sum_{n\in\mathbf{Z}}\mathcal{R}_{\omega,\mathbf{q}}(2nL-x'-x),\qquad(16)$$

where $\mathcal{R}$ the diffusion kernel in an infinite domain:

$$\mathcal{R}_{\omega,\mathbf{q}}(x,x')=\frac{\exp(-\sqrt{q^2+i\,l_\omega^{-2}}|x-x'|)}{2\kappa\sqrt{q^2+i\,l_\omega^{-2}}},\qquad(17)$$

with $\sqrt{-1}\equiv i$. Performing sum (16) and taking the derivative with respect to x yields

$$\partial_x \mathcal{R}^>_{\omega,\mathbf{q}}(0,x')=\frac{\sinh[\sqrt{(qL)^2+i(L/l_\omega)^2}(1-x'/L)]}{\kappa\sinh[\sqrt{(qL)^2+i(L/l_\omega)^2}]}.\qquad(18)$$

A simpler calculation can be carried out if the source is in the negative x region $(x'<0)$. In this case the only image source is symmetric in the $x=0$ plane of the original source, so that the response of the field gradient on the $x=0^-$ side of the plate is described by

$$\partial_x \mathcal{R}^<_{\omega,\mathbf{q}}(0,x')=\frac{e^{-\sqrt{(qx')^2+i(x'/l_\omega)^2}}}{\kappa}.\qquad(19)$$

A. Localized periodic shaking

If the only driving is a single monochromatic shaker located between the plates at $x=x_s$,

$$\eta=\eta_s a^d\delta(x-x_s)\delta(\mathbf{r})\cos(\omega_s t),\qquad(20)$$

then the general expression of the net force acting on the $x=0$ plate is simply obtained from the definition of the response function $\partial_x \mathcal{R}^>$:

$$F(t)=\frac{-\kappa(\eta_s a^d)^2}{4}\left[\int_{\mathbf{q}}|\partial_x \mathcal{R}^>_{\omega_s,\mathbf{q}}(0,x_s)|^2\right][1+\cos(2\,\omega_s t)],\qquad(21)$$

with the short-hand notation $\int_{\mathbf{q}}\equiv\int d\mathbf{q}/(2\pi)^{d-1}$ [24].

There is obviously no force on the left side of the plate, so that using (18) we obtain the exact expression for the instantaneous force on this plate. Its time average $F^>_A$ describes a repulsion between the plates:

$$F^>_A(x_s,\omega_s)=-\frac{(\eta_s a^d)^2}{\kappa L^{d-1}}Y_A\left(\frac{x_s}{L},\frac{L}{l_{\omega_s}}\right)\qquad(22)$$

with

$$Y_A(u,v)=\frac{1}{4}\int_{\mathbf{q}}\left|\frac{\sinh[\sqrt{q^2+iv^2}(1-u)]}{\sinh(\sqrt{q^2+iv^2})}\right|^2.\qquad(23)$$

We now give a closer look at the asymptotics corresponding to the fast and slow shaking limits.

Quasistatic shaking. We first consider the regime where the driving period is much larger than the relaxation time of any interplate field deformation, i.e., the dynamical length is much larger than the interplate distance $(L/l_{\omega_s}\ll 1)$.

The limiting value $Y_A(u,0)$ can be exactly computed by integrating over the in-plane $\mathbf{q}$ modes before summing up all the contributions from all images in Eqs. (16) and (21). If $d=3$ $Y_A(u,0)=\partial_u[\pi(1-u)\cot(\pi u)-2\Gamma u+2(1-u)\psi(u)]/(32\pi)$, with ψ the Euler ψ function, and Γ the Euler constant [25], if $d=2$, $Y_A(u,0)=[1+\pi(1-u)\cot(\pi u)]/(8\pi)$, and if $d=1$, $Y_A(u,0)=(1-u)^2/4$. The scaling function $Y_A(x_s/L,0)$ is plotted in Fig. 7 (log-log plot). The fast decay for values of x_s/L larger than $\frac{1}{2}$ witnesses that the elastic distortions are essentially occurring in the $L/2<x<L$ region.
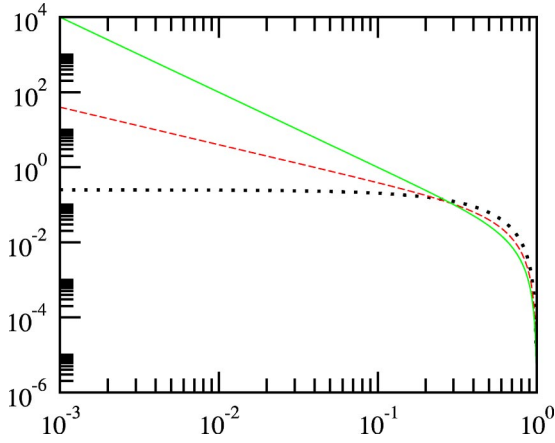
FIG. 7. Log-log plot of the scaling function $Y_A(x_s/L,0)$ vs x_s/L. This corresponds to case A in the quasistatic limit $L/l_{\omega_s} \ll 1$. The full line corresponds to $d=3$, the dashed one corresponds to $d=2$, and the dotted line corresponds to $d=1$.

FIG. 8. Log-linear plot of the scaling function $\tilde{Y}_A$. The full line corresponds to $d=3$, the dashed line to $d=2$, and the dotted line to $d=1$.

Conversely, a shaker close to $x=0$ induces strong variations of the elastic field in the vicinity of the plate, leading to an algebraic divergence of the force when $x_s/L \to 0$ (if $d>1$).

The force dependence on the shaker position can also be qualitatively understood, thanks to an electrostatic analogy. In the present quasistatic limit, the kernel $\mathcal{R}_{\omega_s}^>$ corresponds to the inverse of the Laplace operator (with DBC on the plates). Consequently, ϕ plays the role of an electrostatic potential, the plates mimic a grounded planar capacitance, and the shaking source a point-like particle bearing a charge $\eta_s a^d$. The force on the plate is then analogous to the electrostatic force produced by a pointlike charge [26]. From the image expansion (16) we know that this force is identical to that produced on a virtual plane at $x=0$ by an infinite number of $(+\eta_s a^d)$ charges located at $x=2nL+x_s$ and of $(-\eta_s a^d)$ charges at $x=2nL-x_s$. Hence we have the following conclusions.

(1) If $x_s < L$ (cf. Fig. 6): the electric field on the plate surface is dominated by the image charges at $|x|=x_s$, so $F \sim -(\eta_s a^d)^2/(\kappa x_s^{d-1})$. Higher-order reflections produce image sources that form dipoles viewed from $x=0$. Their subdominant contributions to the electrostatic force actually reduce the above estimation. This implies that the further the second plate, the bigger the force produced by a single shaker.

(2) If $x_s \sim L$ (cf. Fig. 6): the image charges form dipoles located at $x=(2n+1)L$. The electric field on the plate is dominated by the influence of the dipole located at $|x|=L$ (the closest from the $x=0$ plate). The force therefore scales $F_A^> \sim -(\eta_s a^d)^2(1-x_s/L)^2/(\kappa L^{d-1})$.

Fast shaking. If $L/l_{\omega_s} \ll 1$, the electrostatic analogy only provides a partial description of the force generation. In this case, only the first reflexion contribute substantially to the image expansion (16) as if the second plate (at $x=L$) was pushed to infinity. The only remaining length scales are x_s and l_{ω_s}, and the average force can be approximated by

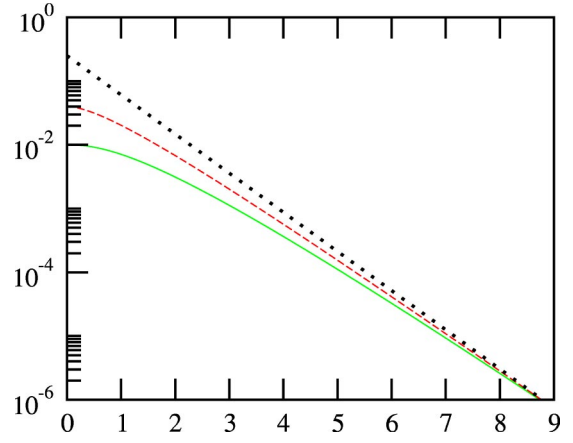$$F_A^> \sim -\frac{(\eta_s a^d)^2}{\kappa x_s^{d-1}}\tilde{Y}_A(x_s/l_{\omega_s}), \qquad (24)$$

with $\tilde{Y}_A(u)=\frac{1}{4}\int_{\mathbf{q}}|\exp(-\sqrt{q^2+iu^2})|^2$. This dimensionless screening factor is plotted in Fig. 8. If the dynamic length l_{ω_s} is larger than the distance separating the shaking source from the plate, $x_s/l_{\omega_s} \gg 1$, the amplitude of the elastic field excitations are exponentially reduced before reaching the plate's surface. More precisely, in this regime,

$$\tilde{Y}_A(u) \sim (u)^{(d-1)/2}\exp(-\sqrt{2}u). \qquad (25)$$

Oppositely, $\tilde{Y}_A(x_s/l_{\omega_s})$ has a nonvanishing finite limit if x_s/l_{ω_s} goes to zero. $F_A^>$ then corresponds to the electrostatic force acting on a conducting plate facing a single "effective" charge $\eta_s a^d$ located at $(x=x_s, \mathbf{r}=0)$, so that, as in the quasistatic case above, $F_A^> \propto -(\eta_s a^d)^2/(\kappa x_s^{d-1})$.

Fluctuations of the shaking-induced force. Beyond the definition and the characterization of the average interplate interaction, it is crucial to notice that the present shaking-induced force is a time varying quantity. Rewriting Eq. (21) as $F(t)=F_A^>[1+\cos(2\omega_s t)]$, it is obvious that the force experienced by the immersed plates cannot be *a priori* reduced to its sole average value. As a matter of fact the fluctuations of the instantaneous force are comparable to its average amplitude.

B. Homogenous monochromatic shaking

We now consider that the soft medium is uniformly shaken by $\eta(\vec{R},t)=\eta_s\cos(\omega_s t)$. η is the superposition of in-phase shakers of the $-A-$ type uniformly distributed in space. All the elementary shakers produce periodic elastic deformations that "interfere" and give rise to the instantaneous forces $F^>(t)$ [respectively $F^<(t)$] at $x=0^+$ (respectively $x=0^-$) obtained from Eqs. (2) and (6):

$$F^>(t)=-\frac{\kappa}{4}L_\parallel^{d-1}\left|\int_0^L \partial_x \mathcal{R}_{\omega_s,\mathbf{0}}^>(0,x')dx'\right|^2$$

$$\times[1+\cos(2\omega_s t+\theta^>)], \qquad (26)$$

with $\theta^> = 2 \arg[\int_0^L \partial_x \mathcal{R}^>_{\omega_s,0}(0,x')dx']$, and

$$F^<(t) = \frac{\kappa}{4} L_\parallel^{d-1} \left| \int_0^\infty \partial_x \mathcal{R}^>_{\omega_s,0}(0,x')dx' \right|^2$$
$$\times [1 + \cos(2\omega_s t + \theta^<)], \tag{27}$$

with $\theta^< = 2 \arg[\int_0^\infty \partial_x \mathcal{R}^<_{\omega_s,0}(0,x')dx']$. At every instant these two forces compete. They push the plate in opposite directions to give rise to the net force $F(t)$. The latter is exactly computed using Eqs. (3), (18), (19), (26), and (27), and after some elementary algebra [24]:

$$F(t) = F_B \left[1 + \frac{\cos(2\omega_s t)}{\cos[L/(\sqrt{2}l_{\omega_s})]} \right]. \tag{28}$$

The average F_B is given by

$$F_B = \frac{\eta_s^2 L_\parallel^{d-1}}{\kappa} l_{\omega_s}^2 Y_B \left(\frac{L}{l_{\omega_s}} \right), \tag{29}$$

$$Y_B(u) = \frac{1}{2} \frac{\cos(u/\sqrt{2})}{\cos(u/\sqrt{2}) + \cosh(u/\sqrt{2})}. \tag{30}$$

The function Y_B is plotted in Sec. III B, see Fig. 4, where its fast and slow asymptotics are qualitatively studied.

Mean force tunability. The tunability of the present shaking-induced force is clearly revealed by Eqs. (29) and (30). Precisely for fixed L (i) the shaking pulsation ω_s sets the sign of F_B to sign$[\cos\{L/(\sqrt{2}l_{\omega_s})\}]$, and its range to $\sim l_{\omega_s}$ [via the cosh term in Eq. (29)], (ii) then η_s allows to adjust the mean force amplitude arbitrarily. This second assertion is actually true only if $L \neq \pi/\sqrt{2}(2n+1)l_{\omega_s}$, with n integer. In such cases the plates experience no mean net force.

Fluctuations of the shaking-induced force. Equation (28) indicates actually that $F(t)$ "fluctuates" periodically around F_B with a pulsation $2\omega_s$. Moreover, the amplitude of the $2\omega_s$ components of the force is $1/\cos[L/(l_{\omega_s}\sqrt{2})]$ times larger than its mean value F_B, whatever the shaking parameters ω_s and η_s.

Shaking-induced organization. The two preceeding comments strongly suggest that the homogenous shaking may be used to dynamically induce spacial "localization" of the plates. As a matter of fact, when mesoscopic objects are immersed in a soft medium, their intrinsic dynamics (ignored in the present work) necessarily filters out high frequency effects of external forcing. If their response time is much larger than $1/(2\omega_s)$, these "slow" moving objects only respond to the stationary component F_B of the shaking-induced force. The corresponding steady-state interplate distance in the present simple geometry is then controllable by tuning ω_s.

C. Colored noisy shaking

The medium surrounding the plates is now supposed to be driven by stochastic shaking sources with zero mean and mean-squared fluctuations given by Eq. (13). The noise av-

eraged net force F_C experienced by the plate at $x = 0$ is the sum of the mean values of the two independent forces $F^>$ and $F^<$. Using Eqs. (12),(18),(20) this force is written as

$$F_C = \frac{2L_\parallel^{d-1}}{a^d} \int_\omega S_\omega \left[\int_0^L [F_A^>(x,\omega) + F_A^<(-x,\omega)]dx \right.$$
$$\left. + \int_L^\infty F_A^<(-x,\omega)dx \right]. \tag{31}$$

Exact results. For a Lorentzian power spectrum, see Eq. (14), the integration over frequency and position of all the elementary contributions $F_A(x,\omega)$ in Eq. (31) yields

$$F_C = \frac{\eta_s^2 a^d L_\parallel^{d-1}}{\kappa L^{d-2}} Y_C \left(\frac{L}{l_{\Omega_s}} \right), \tag{32}$$

$$Y_C(u) = \frac{1}{4u^2} \int_\mathbf{q} q(\coth q - 1)$$
$$- \frac{1}{4u^2} \int_\mathbf{q} \sqrt{q^2 + u^2}[\coth(\sqrt{q^2 + u^2}) - 1]. \tag{33}$$

The scaling function Y_C is plotted in Fig. 5. To achieve the exact computation of F_C, the integral over the in-plate $\mathbf{q}$ modes in Eq. (33) is performed. After some algebra we obtain, if $d = 1$, $Y_C = \{1 - u[\coth(u) - 1]\}/u^2$, if $d = 3$, $Y_C = [3\zeta(3) - \pi^2 - 6u^2 - u\log(1 - e^{2u}) + 3\text{Li}_2(e^{2u})]/(48\pi u^2)$, where ζ is the Riemann ζ function and Li_2 the dilogarithm function, $\text{Li}_2(x) = \Sigma_{k=1}^\infty x^k/k^2$. Finally for the $d = 2$ case $Y_C = 2\Sigma_n[K_0(2nu) + K_2(2nu)]$, where K_n is the nth K-Bessel function [25].

Notice that this last calculation can actually be bypassed, if one already knows the thermal Casimir force the left plate would feel if the soft medium had a finite correlation length ξ, precisely if the elastic Hamiltonian were $\mathcal{H} = (\kappa/2)\int[[\vec{\nabla}\phi(\vec{R})]^2 + [\phi(\vec{R})/\xi]^2]d^d\vec{R}$. Denoting this force $\tilde{F}_{\text{Casimir}}(L/\xi)$, we can show that Eqs. (32) and (33) can be recast into [27]

$$F_C = \frac{\eta_s^2 a^d \Omega_s^{-1}}{2\gamma k_B T} \left[\tilde{F}_{\text{Casimir}}(0) - \tilde{F}_{\text{Casimir}} \left(\frac{L}{l_{\Omega_s}} \right) \right], \tag{34}$$

where $\tilde{F}_{\text{Casimir}}(0)$, of course, corresponds to the Casimir force the plate experiences in a scale-free fluctuating medium, cf. Eq. (8).

Qualitative approach. Equation (31) shows clearly that F_C is the result of the incoherent sum over frequencies and positions of the forces produced by localized shakers of the $-A-$ type. Note that the sum over the shaking frequencies is weighted by the noise power spectrum S_ω. This decomposition is now used to justify first the sign of the mean force, then the algebraic decays of the mean force as observed in Eq. (32) and Fig. 5.

Only the elementary monochromatic shakers localized at distances $|x| < L$ on the left-hand side of the plate have a

challenger in the $0<x<L$ inner region. Referring to the discussion in Sec. IV A, we know that $F_A^<>0$ and that $|F_A^>(x,\omega)|<|F_A^<(-x,\omega)|$. Moreover, S_ω is necessarily a positive quantity for all frequencies. It then turns out that the net mean force is positive, for any choice of S_ω, the two objects attract each other. Besides, $F_A^>(x,\omega) \sim -F_A^<(-x,\omega)$ for shaker located at $x<L/2$. This important property leads to the cancellation of the short-distance divergences in the first term of Eq. (31). Finally, $|F_A^>(x,\omega)| \ll |F_A^<(-x,\omega)|$ if $|x|>L/2$, so that Eq. (31) can be approximated by $F_C \sim 2L_\parallel^{d-1}a^{-d}\int_\omega S_\omega \int_{L/2}^\infty F_A^<(-x,\omega)dx$.

To sum up, the elastic field deformations produced by the $-A-$ type shakers located at $x<-L/2$ dominate the mean net force F_C.

Without refering to any specific choice for S_ω, the noise power spectrum is here characterized only by its width Ω_s, see, e.g., Eq. (13). Thus, going to the (x,l_ω) variables and defining $L^* \equiv \max(L,l_{\Omega_s})$ we easily deduce

$$F_C \sim \frac{\eta_s^2 a^d \Omega_s^{-1} L_\parallel^{d-1}}{\gamma} \int_{L^*}^\infty \frac{dl_\omega}{l_\omega^3} \int_L^{l_\omega} \frac{dx}{x^{d-1}}, \quad (35)$$

since $F_A^<(x,\omega)$ is exponentially weak if $x>l_\omega$ and scales as $1/x^{d-1}$ if $x<l_\omega$, cf. Fig. 8.

We can now integrate (35) and distinguish the two cases.

(i) $L/l_{\Omega_s} \gg 1$. In this wide noise spectrum limit $F_C \sim (\eta_s^2 a^d \Omega_s^{-1}/\gamma)L_\parallel^{d-1}/L^d$, the thermal Casimir force scaling is obtained as anticipated in Sec. III.

(ii) $L/l_{\Omega_s} \ll 1$. In this case the noise correlation time $\sim \Omega_s^{-1}$ is larger than the field relaxation over distances smaller than L. The number of elementary shakers contributing to the force is substantially increased compared to (1). Depending on the space dimension d, we obtained the three scaling forms: if $d=3$, $F_C \sim (\eta_s^2 a^3 \kappa^{-1})L_\parallel^2/L$; if $d=2$, $F_C \sim (\eta_s^2 a^2 \kappa^{-1})L_\parallel \log(l_{\Omega_s}/L)$; an finally if $d=1$, $F_C \sim (\eta_s^2 a \kappa^{-1})l_{\Omega_s}$. In agreement with the above exact calculations and with Fig. 5.

Fluctuations of the shaking-induced force. To conclude this section, we address briefly the question of the fluctuations of the force. In order to asses their relative importance with respect to the mean force value, we introduce the dimensionless ratio $F_C/\Delta F$, where the mean-squared deviation ΔF^2 is defined by $\Delta F^2 \equiv \langle F(t)^2 \rangle - F_C^2$. Whereas F_C is the result of the competition between the mean forces $F_C^>$ and $F_C^<$ of opposite signs, the forces' fluctuations on the two sides add up and $\Delta F^2 = (\Delta F^>)^2 + (\Delta F^<)^2$ with obvious notations. Note that the noise's four points correlation function is *a priori* required to compute ΔF. We make here one more assumption and consider that $\eta(\vec{R},t)$ are Gaussian random variables with correlations given by Eqs. (13) and (14). This allows to fully characterize the shaking process and, consequently, the variance of the shaking-induced force. For the sake of clarity we present without additional details the scaling form of the mean over variance ratio (ignoring logarithmic corrections):

$$\frac{F_C}{\Delta F} \sim \left(\frac{L_\parallel}{L}\right)^{(d-1)/2} \begin{cases} \left(\dfrac{L}{l_{\Omega_s}}\right)^{(3-d)/2} & \text{if } L/l_{\Omega_s} \ll 1 \\[12pt] \left(\dfrac{l_{\Omega_s}}{L}\right)^{(d+1)/2} & \text{if } L/l_{\Omega_s} \gg 1, \end{cases} \quad (36)$$

we have also assumed $d>1$, since the one-dimensional case deserve a more careful analysis as in the equilibrium context more carefully studied in Ref. [27]. The above expressions show that the present shaking-induced force cannot be *a priori* reduced to its sole value F_C. Indeed, depending on the geometrical aspect ratio $L_\parallel/L$ and on the noise correlation time Ω_s^{-1} the variance of the force can dominate its mean value by orders of magnitude.

D. Toward more complex dynamics

To what extent do the results presented above apply to systems evolving according to more complex dynamics? It is noticeable that only the explicit form of the scaling functions Υ_X requires a precise description of the field dynamics. Conversely, all the qualitative analysis as well as the asymptotic expressions for the various forces involve only the definition of the dynamical length l_ω. We thus expect that they should be extendable to any other dynamic scheme relating algebraically the spatial and the temporal relaxation scale.

V. SUMMARY AND OUTLOOK

To summarize, a simple model has allowed us to show that the concept of fluctuation-induced interactions can be extended to complex fluids driven to out of equilibrium. Our main result concerns identical platelike inclusions immersed in an homogenous medium externally driven by $-A-$, a monochromatic localized shaking source located between the plates, $-B-$, a monochromatic and homogenous shaking and $-C-$, a noisy colored shaking. These external processes generate effective forces on the plates without acting directly on them. The main features of the mean forces induced by these three simple shaking are summarized in the table below and compared to their equilibrium thermal Casimir analog.

Shaking	Amplitude	Range	Sign
A	η_s^2	l_{ω_s}	repulsion
B	η_s^2	l_{ω_s}	tunable
C	η_s^2	power law	attraction
Thermal	$k_B T$	power law	attraction

Five points are worth highlighting.

(i) Although a shaking at a single frequency leads necessarily to short-range interactions, noisy shakings generate effective forces that decays algebraically with the interplate distance.

(ii) If the external shaking occurs only between the two plates the resulting interaction is always repulsive. Conversely, when distributed on the whole sample the external

shakers generate forces on both sides of the plates. The resulting net force is attractive for spatially uncorrelated shaking. On the contrary, with coherent shaking, interference phenomena between the elastic medium distortions can lead to attractive or repulsive interactions.

(iii) The soft medium-plates coupling has been here modeled by Dirichlet boundary conditions. As in the equilibrium case our results are expected to hold for other static boundary conditions representing strong interactions. In contrast the description of situations of weaker coupling and/or cases where dynamic boundary conditions are required could yield to new phenomenology.

(iv) The generalization of our results to an elastic medium characterized by an intrinsic relaxation scale ξ [see the discussion above Eq. (34)] can be done without much effort following blindly the procedures described in this paper. The only qualitative difference in the results summarized in the above table is the forces' range. For shakings of the $-A-$ and $-B-$ type the range of the force becomes $\min(\xi, l_\omega)$. In the noisy shaking case $-C-$ the force decay is not algebraic anymore but exponential for interplate distances larger than ξ.

(v) Beyond the derivation of their average values, we have also shown that the shaking-induced forces are in general expected to be strongly fluctuating quantities, whatever their precise origin.

To conclude, let us recall that our description is clearly extremely simplified and of course is not supposed to model any real system. Even within this simple framework the extension of our result to many moving objects remains complex. But, the analysis of simplified situations such as that described here could certainly help understand ordering and dynamic behavior of inclusions in out-of-equilibrium complex fluids.

---

[1] D. Frenkel, in *Soft and Fragile Matter: Nonequilibrium Dynamics, Metastability and Flow*, edited by M.E. Cates and M.R. Evans (IOP Publishing, Bristol, 2000), and references therein.

[2] P. Poulin, H. Stark, T.C. Lubensky, and D.A. Weitz, Science (Washington, DC, U.S.) **275**, 1770 (1997).

[3] R. Netz and P. Pincus, Phys. Rev. E **52**, 4114 (1995); I. Koltover, J.O. Radler, and C.R. Safinya, Phys. Rev. Lett. **82**, 1991 (1999).

[4] B.V. Derjaguin and L. Landau, Acta Physicochim. URSS **14**, 633 (1941); E.J. Verwey and J.T.G. Overbeek, *Theory of the Stability of Lyophobic Colloids* (Elsevier, Amsterdam, 1948).

[5] L. Onsager, Ann. N.Y. Acad. Sci. **51**, 627 (1949).

[6] A. Ajdari, L. Peliti, and J. Prost, Phys. Rev. Lett. **66**, 1481 (1991).

[7] M. Kardar and R. Golestanian, Rev. Mod. Phys. **71**, 1233 (1999), and references therein.

[8] H.B.G. Casimir, Proc. K. Ned. Akad. Wet. **51**, 793 (1948).

[9] G.A. Voth, B. Bigger, M.R. Buckley, W. Losert, M.P. Brenner, H.A. Stone, and J.P. Gollub, Phys. Rev. Lett. **88**, 234301 (2002).

[10] B.A. Grzybowski and G.M. Whitesides, Science (Washington, DC, U.S.) **26**, 718 (2002).

[11] S. Ramaswamy, J. Toner, and J. Prost, Phys. Rev. Lett. **84**, 3494 (2000).

[12] S.H. Behrens and D.G. Grier, in *Electrostatic Effects in Soft Matter and Biophysics*, edited by C. Holm, P. Kekicheff, and R. Podgornik (Kluwer, Dordrecht, 2001).

[13] T.M. Squires and M.P. Brenner Phys. Rev. Lett. **85**, 4976 (2000).

[14] M.B. Hastings, Z.A. Daya, E. Ben-Naim, and R.E. Ecke, Phys. Rev. E **66**, 025102 (2002).

[15] P.G. de Gennes, Rev. Mod. Phys. **57**, 827 (1985).

[16] P.-G. de Gennes and J. Prost, *The Physics of Liquid Crystals* (Clarendon, Oxford, 1993).

[17] A. Boudaoud, Y. Couder, and M. Ben Amar, Eur. Phys. J. B **9**, 159 (1999).

[18] P.G. de Gennes, F. Brochard-Wyart, and D. Quere, *Goutes, Bulles, Perles et Ondes* (Belin, Paris, 2002).

[19] P.-G. de Gennes and J. Prost, *The Physics of Liquid Crystals* (Clarendon, Oxford, 1993), p. 135–139.

[20] L.D. Landau and E.M. Lifshitz, *The Classical Theory of Fields,* 4th ed. (Pergamon, Oxford, England, 1975).

[21] L. LeGoff, F. Amblard, and E. Furst, Phys. Rev. Lett. **88**, 018101 (2002).

[22] H. Li and M. Kardar, Phys. Rev. Lett. **67**, 3275 (1991).

[23] Phillip McCord Morse and Herman Feshbach, *Methods of Theoretical Physics* (McGraw-Hill, New York, 1953).

[24] The phase shift with respect to the original shaking process has been ignored for the sake of clarity.

[25] I.S. Gradstein and I.M. Ryzhik, *Table of Integrals, Series and Products* (Academic Press, San Diego, 1987).

[26] J.D. Jackson, *Classical Electrodynamics* (Wiley, New York, 1999).

[27] D. Bartolo, A. Ajdari, J.-B. Fournier, and R. Golestanian, Phys. Rev. Lett. **89**, 230601 (2002).